CHALMERS
UNIVERSITY OF TECHNOLOGY

Microcapsule functionalization enables rate-determining release from cellulose nonwovens for long-term performance

Citation for the original published paper (version of record):
Eriksson, V., Mistral, J., Yang Nilsson, T. et al (2023). Microcapsule functionalization enables rate-determining release from cellulose nonwovens for long-term performance. Journal of Materials Chemistry B, 11(12): 2693-2699. http://dx.doi.org/10.1039/d2tb02485c

Journal of Materials Chemistry B

ROYAL SOCIETY OF CHEMISTRY

PAPER

View Article Online
View Journal

Cite this: DOI: 10.1039/d2tb02485c

Microcapsule functionalization enables rate-determining release from cellulose nonwovens for long-term performance†

Viktor Eriksson, [a] Jules Mistral, [ab] Ting Yang Nilsson, [c] Markus Andersson Trojer [c] and Lars Evenäs *[ad]

Received 14th November 2022,
Accepted 13th February 2023

DOI: 10.1039/d2tb02485c

rsc.li/materials-b

Functional textiles is a rapidly growing product segment in which sustained release of actives often plays a key role. Failure to sustain the release results in costs due to premature loss of functionality and resource inefficiency. Conventional application methods such as impregnation lead to an excessive and uncontrolled release, which – for biocidal actives – results in environmental pollution. In this study, microcapsules are presented as a means of extending the release from textile materials. The hydrophobic model substance pyrene is encapsulated in poly(D,L-lactide-*co*-glycolide) microcapsules which subsequently are loaded into cellulose nonwovens using a solution blowing technique. The release of encapsulated pyrene is compared to that of two conventional functionalization methods: surface and bulk impregnation. The apparent diffusion coefficient is 100 times lower for encapsulated pyrene compared to impregnated pyrene. This clearly demonstrates the rate-limiting barrier properties added by the microcapsules, extending the potential functionality from hours to weeks.

1. Introduction

Release of active substances in general and sustained release in particular is important in many industrial sectors. These range from the delivery of drugs in pharmaceutical formulations and medical devices to biocides used for antifouling purposes or pesticides used in agriculture.[1–5] Taking (micro)biological control in *e.g.* wound care, antifouling, or plant protection as illustrative examples; a slow and continuous release removes the need for using larger doses to maintain an effective concentration of active substance over time. The problems with inadequate control of the release are originating from the resulting very high initial release rates. Such a release profile leads to a premature loss of activity as the released concentration quickly decreases below the minimum efficient concentration. A conventional countermeasure to prolong the activity is to simply increase the dosage. However, this results in a considerable waste of actives – far above the minimum efficient concentration. This causes pollution of the surrounding environment followed by release of actives below the minimum efficient concentration over a long time span which for antimicrobial actives drives antimicrobial resistance development.[6,7]

A means to control the release of the actives, and thus means to avoid the issues stated above associated with uncontrolled release, is to encapsulate them into delivery vehicles. Several delivery vehicles for achieving sustained release are presented in the literature, including mesoporous silica nanoparticles[8,9] and polymeric microcapsules[2,5] among others. For the last decades, polylactides have been used extensively as biodegradable microcapsule materials.[10,11] This family of polymers can be produced from renewable resources and degrade into safe degradation products, making them attractive alternatives as microcapsule materials.[12,13]

In many applications, sustained release is desired from a macroscopic object such as a paint film or an implant where the microparticles are embedded in for example a coating matrix or a hydrogel.[14–16] An additional and growing product segment is functional fiber materials, ranging from textiles in agriculture and ropes or nets for marine applications to wound dressings, implants, and fibrous scaffolds for tissue engineering.[17] Fibers are, as compared to coatings and hydrogels, generally more difficult to functionalize with microcapsules – especially polymeric capsules that are biobased and thermosensitive[18] when compared

[a] Department of Chemistry and Chemical Engineering, Chalmers University of Technology, 412 96, Gothenburg, Sweden. E-mail: lars.evenas@chalmers.se
[b] Univ Lyon, CNRS, UMR 5223, Ingénierie des Matériaux Polymères, Université Claude Bernard Lyon 1, INSA Lyon, Université Jean Monnet, F-69622, Villeurbanne Cédex, France
[c] Department of Polymers, Fibers and Composites, Fiber Development, RISE, 431 53, Mölndal, Sweden
[d] Wallenberg Wood Science Center, Chalmers University of Technology, 412 96, Gothenburg, Sweden

† Electronic supplementary information (ESI) available. See DOI: https://doi.org/10.1039/d2tb02485c

to inorganic particles. The use of biobased capsules does, however, add value to the materials by allowing the design of systems based on renewable resources and that can be biodegraded. Given the current trends toward a circular economy and biobased materials, regenerated fibers from the most abundant biopolymer cellulose are interesting for these functional fiber materials.[19] Several methods are available for preparing different types of fiber materials based on regenerated cellulose. The most well-known techniques for preparing continuous regenerated cellulosic fibers are the viscose and lyocell wet-spinning processes.[19,20] If instead nonwovens are desired, electrospinning is a popular approach where nanoparticle functionalization previously has been studied.[21,22] Noteworthy here is solution blowing, which has recently been proposed as an alternate way of producing cellulose nonwovens, addressing the problems of upscaling associated with electrospinning.[23–25] Compared to fossil based fiber materials, spinning fibers from regenerated cellulose often requires harsh chemicals, further complicating any functionalization by microcapsules. We have recently published a paper describing a wet-spinning and corresponding solution blowing method that allows for a range of microcapsules to be efficiently incorporated into continuous textile filaments or nonwovens based on different biobased polysaccharides.[18]

The sustained release from particles in the nanometer range is usually fast and complete within hours to days due to short diffusional pathways. This is especially true for inorganic nanoparticles onto which the actives are physiosorbed (such as in the nanoparticle-functionalized electrospun fibers mentioned above). In such a case, the diffusivity barrier added by the fiber matrix would also affect the release to a significant amount, leading to difficulties in predicting and controlling the release profile. In addition, any swelling of the fiber would affect the release profile. It is instead desirable to have a controlled release system that is rate-determining. This would completely decouple the release properties of the fiber matrix from the produced release profile, leading to improved predictability and control by tuning the microparticle size.

In this work, we demonstrate how the microcapsule barrier properties dominate, and therefore facilitate the control of, the release rate from cellulosic nonwovens. The model substance pyrene has been loaded into solution blown cellulose fibers in three different ways: (i) surface impregnation, (ii) bulk impregnation, and (iii) microencapsulation into microcapsules embedded within the fibers. Following this, the release of pyrene from these materials has been investigated and fitted with Fickian diffusion models to determine the apparent diffusion coefficients of pyrene and hence the barrier properties of the materials.

2. Experimental section

Avicel PH-101 (MCC), Brij L23, dichloromethane (DCM $\geq$ 99.9%), methanol (MeOH, $\geq$99.9%), 1-ethyl-3-methylimidazolium acetate (EMIMAc, 95%), pyrene ($\geq$99.0%) and (3-(4,5-dimethylthiazol-2-yl)-2,5-diphenyltetrazoliumbromid) (MTT) were purchased from Sigma-Aldrich. Acetone ($\geq$99.8%, VWR Chemicals), ethanol (EtOH, 99.5%, Solveco), poly(D,L-lactide-*co*-glycolide) (PLGA, 70 : 30 L : G, M_w 10 kDa, Polysciences Inc.) and poly(vinyl alcohol) (PVA, 95% hydrolyzed, M_w 95 kDa, Acros Organics) were also used. Eagle's minimum essential medium with Earle's balanced salt solution buffered with $NaHCO_3$, non-essential amino acids, stable glutamine, fetal bovine serum and trypan blue stain were purchased from Gibco Life Technologies. Sodium pyruvate, penicillin-streptomycin, trypsin-EDTA and DPBS without Ca^{2+} were purchased from GE Healthcare HyClone. All chemicals were used as received. Unless otherwise specified, water of MilliQ quality (resistivity $\geq$ 18 MΩ cm) was used.

2.1 Microsphere formulation

Microspheres were formulated according to a modified solvent evaporation technique previously used by us.[26] The core oil was replaced by an equal amount of PLGA to produce microspheres rather than core–shell particles. PLGA (0.133 g) and pyrene (4 mg) were dissolved in DCM (3.2 mL) and acetone (200 μL), which was added slowly over 2 minutes to an aqueous phase containing 1 wt% PVA dispersant (2.5 mL). This was done while homogenizing at 4000 rpm with a Kinematica PT3100D homogenizer equipped with dispersing aggregate PT-DA07/2EC-F101. After 60 minutes of homogenization, the formed emulsion was diluted with an additional volume of aqueous phase (2.5 mL) and left under gentle stirring at 300 rpm overnight for the volatile solvents to evaporate.

2.2 Solution blowing

The cellulose dope solution for the solution blowing was prepared by drying MCC at 80 °C for one hour.[18,24] The dried MCC was then added to EMIMAc while overhead-stirring at 150 rpm to yield an MCC concentration of 9 wt%. The solution was heated to 70 °C and stirred for one hour for the cellulose to dissolve, after which the solution was cooled down to room temperature. For fibers containing bulk impregnated pyrene, an amount equal to 0.12 wt% of the cellulose was added from a stock solution of pyrene in EMIMAc (2 mg mL^{-1}). For fibers containing microspheres, the prepared microsphere suspension was centrifuged to remove excess water at 1000 and 2000 rpm for 5 minutes each, collecting the sediment after each run. The sedimented microspheres were redispersed in EMIMAc and added dropwise to the cooled-down dope solution under vigorous stirring. Finally, the dope solution was centrifuged at 1000 rpm to remove air bubbles.

Solution blowing was performed at room temperature in a Biax-Fiberfilm solution blowing spinneret containing 9 nozzles of 220 μm diameter. The spinneret was connected to a cylinder pump set to an extrusion speed of 2.5 mL min^{-1} and pressurized air at 0.3 bar. The solution was sprayed onto a rotating drum immersed in a deionized water coagulation bath where the nonwoven cellulose was collected. Following solution blowing, the nonwoven was thoroughly washed in deionized water to remove residual EMIMAc.

Samples for surface impregnation of pyrene were prepared by solution blowing pure cellulose fibers. After washing and drying the nonwovens, a solution of pyrene in DCM was added

dropwise at 2 mL g^{-1} cellulose. This was just below the maximum amount of liquid that the nonwovens could hold without anything dripping from the material. Finally, the DCM was allowed to evaporate completely overnight in a fume hood.

2.3 Optical microscopy

Optical microscopy was used to characterize the prepared nonwoven fiber materials. Tiny bundles of fibers were placed in immersion oil on an object glass before analysis in a Zeiss Axio Imager Z2m using both brightfield and differential interference contrast techniques. Fluorescence imaging was performed by using an HBO lamp and filter set 49 for pyrene.

2.4 Confocal microscopy

Confocal micrographs of cellulose fibers containing pyrene-loaded PLGA microspheres were captured using a confocal laser scanning microscope (Nikon Ti-E/A1+) with excitation at 405 nm. Images were collected every 0.1 μm along the *z*-axis. The fibers were placed in immersion oil on an object glass before analysis.

2.5 Scanning electron microscopy

Tiny bundles of fibers were immersed in liquid nitrogen and while cooled broken off with a pair of tweezers to obtain fresh cross-sections. The fibers were then mounted on conducting holders using a conducting silver glue and viewed in a Zeiss LEO 55 scanning electron microscope using secondary electron detection at 1 kV acceleration voltage.

2.6 Release measurements

To quantify the release from the samples, the fibers were immersed in well-stirred aqueous solutions of 6 wt% nonionic surfactant Brij L23, to ensure sink conditions. Aliquots were collected at given times and analyzed using UV-visible spectrophotometry.[26]

The loading efficiency of pyrene in the samples was determined by immersing the fibers in methanol overnight to leach out all pyrene and then determining the pyrene concentrations by UV-visible spectrophotometry.

2.7 UV-Vis spectrophotometry

Quantification of pyrene during the release measurements was performed by UV-vis spectrophotometry. Measurements were performed in 10 mm Hellma quartz cuvettes using an HP 8453 spectrophotometer. The maximum absorption was observed and recorded at 242 nm in the aqueous Brij L23 solution, and a blue shift to 240 nm was observed in MeOH and 3 : 1 EtOH : 6% aq. Brij L23. Calibration curves following the Beer–Lambert law, $A = \varepsilon cl$, for pyrene in water, 3 : 1 EtOH : 6% aq. Brij L23, and MeOH were created (Fig. S2, ESI†).

2.8 Size distributions

Size distributions of the microcapsules both in aqueous suspension and embedded in fibers were determined as described by us previously.[27] For the size distributions of the different fiber materials, the radii were determined by measuring at least 100 points for each sample. All data sets were well-described by lognormal size distributions.

2.9 Diffusion models

The fractional release from a sphere, f_s, at time t is described by Crank[28] as

$$f_s(r,t) = \frac{\alpha_s}{1+\alpha_s}\left(1 - \sum_{n=1}^{\infty} \frac{6\alpha_s(\alpha_s+1)}{9+9\alpha_s+q_{s,n}^2\alpha_s^2} \exp\left(-\frac{Dq_{s,n}^2 t}{r^2}\right)\right) \quad (1)$$

where D is the pyrene diffusion coefficient in a sphere with radius r. The coefficient α_s is defined as

$$\alpha_s = \frac{V_{sink}}{V_{sphere}K}. \quad (2)$$

Here, K is the pyrene partitioning coefficient between release medium and sphere, and V_{sink} and V_{sphere} are their respective total volumes. Finally, $q_{s,n}$ is the n: th non-zero positive root of

$$\tan q_{s,n} = \frac{3q_{s,n}}{3+\alpha_s q_{s,n}^2}. \quad (3)$$

The samples of microcapsules are polydisperse as described by the size distribution $p(r)$. The final expression for the fractional release is then given by

$$\frac{m(t)}{m_{tot}} = \frac{\int f_s(r,t)p(r)r^3 dr}{\int p(r)r^3 dr} \quad (4)$$

where m is the mass of released substance and m_{tot} the total amount in the sphere at time zero. For these systems, the particle radii were well described by a lognormal size distribution as shown in Fig. S1 in the ESI.† Release from microcapsules in both fibers and aqueous suspension was described as diffusion from a spherical geometry, resulting in effective diffusion coefficients D.

By similar means, release from the fiber samples with pyrene either bulk impregnated or encapsulated into microcapsules, could be described by diffusion in a cylindrical geometry. The Fickian diffusion models used here are presented in the ESI.†

2.10 Cytotoxicity

The cytotoxicity of the microsphere-containing cellulose nonwovens was determined according to ISO 10993-5:2009. Extracts from the nonwoven material was collected using culture medium with serum as extraction vehicle for 24 h at 37 °C. In addition to the nonwoven material, a negative (thermanox plastic coverslips form Thermo Scientific NUNC) and a positive control (latex rubber Gammex 91-325 from AccuTech Ansell) with six replicates per material.

L929 mouse fibroblast cells (NCTC clone 929: CCL-1 American Type Culture Collection) were propagated in a tissue culture flask to obtain subconfluent monolayers of cells in a 96 well plate (100 μL/10^4 cells per well). The extracts were added to the six replicate wells containing the subconfluent cell monolayer and the plate was incubated for 24 hours at 37 °C. After the incubation, the extracts were removed and an MTT solution was added to each well after which the plate as incubated for two hours at 37 °C in 5% CO_2. The MTT solutions was subsequently removed, after which 2-propanol was added under rigorous shaking. The viability was finally assessed by

quantifying the resulting formazan product using UV-vis spectrophotometry at 570 nm.

3. Results and discussion

3.1 Material characterization

To begin with, we consider the fabrication and characterization of the three types of nonwovens as shown in Fig. 1; surface impregnated (Fig. 1a), bulk impregnated (Fig. 1b) and microcapsule-functionalized nonwovens (Fig. 1c). A photograph showing the macroscopic appearance of the materials is shown in Fig. S7 in the ESI.† Solution blowing was performed by using a dope solution of microcrystalline cellulose dissolved in the ionic liquid 1-ethyl-3-methylimidazolium acetate. To prepare microcapsules for immobilization within the fibers, poly(D,L-lactide-*co*-glycolide) (PLGA) microcapsules encapsulating pyrene were formulated according to a solvent evaporation technique.[26] The microcapsules were prepared in an aqueous medium and then concentrated by centrifugation. The sediment was collected, added to, and dispersed in the cellulose dope solution prior to solution blowing.

For preparing surface impregnated fibers, pyrene was dissolved in dichloromethane and added dropwise to a cellulose nonwoven material after which the solvent was evaporated rapidly. In this case, pyrene was detected on the surface of the fibers using fluorescence microscopy (Fig. 1a2). A homogeneous film of pyrene was not observed but it was rather found in small and separated areas with larger concentrations of pyrene. Fibers with bulk impregnated pyrene were prepared by dissolving pyrene directly in the dope solution before solution blowing. In this case, homogeneous fluorescence intensity was seen throughout the entire fiber (Fig. 1b2), indicating an even distribution of pyrene. It should also be noted that cellulose exhibits autofluorescence in the same spectral region as pyrene, making it hard to differentiate a low pyrene concentration from cellulose based only on fluorescence micrographs.

In the microcapsule-functionalized fibers, the microcapsules were well-dispersed throughout the entire fiber cross-section (Fig. 1c1 and 2b). Fluorescence micrographs revealed that pyrene was highly partitioned towards the microcapsules rather than the surrounding fiber (Fig. 1c2 and Fig. S5, ESI†). The microcapsules were also seen to remain intact without any fragmentation during the solution blowing process. This was further confirmed by scanning electron microscopy, Fig. 2a. Some fibers appeared to be slightly flattened, most likely a consequence of collecting not fully coagulated fibers onto the rotating drum in the coagulation bath. For all three samples, the fibers were loaded with equal amounts of pyrene. The biocompatibility of microcapsule-functionalized fibers without pyrene was determined. The material was non-cytotoxic towards L929 mouse fibroblast cells as shown in the ESI.†

3.2 Release measurements

We will now consider the release from the three types of nonwovens. To fit the release data with the Fickian diffusion models described below, the materials' dimensions must be

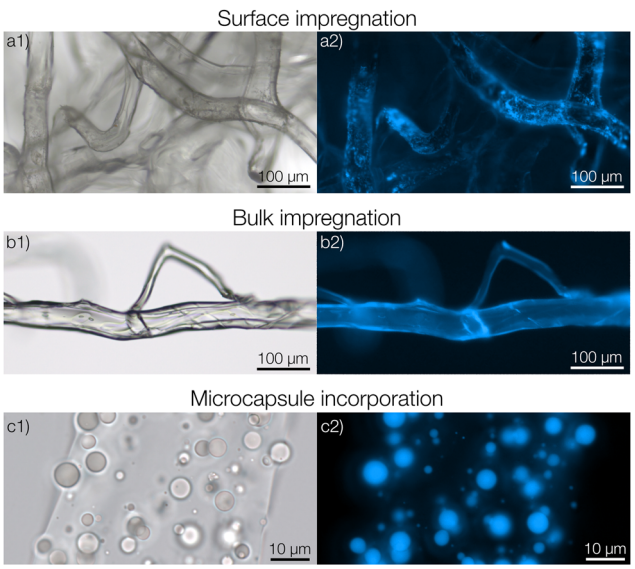

Fig. 1 Three types of functionalized fiber materials with pyrene as an active substance. (a1) Optical micrograph of a fiber with a surface impregnation of pyrene. (a2) Fluorescence micrograph of the same area. (b1 and b2) Fibers with bulk impregnated pyrene. (c1 and c2) Fibers with embedded microcapsules.

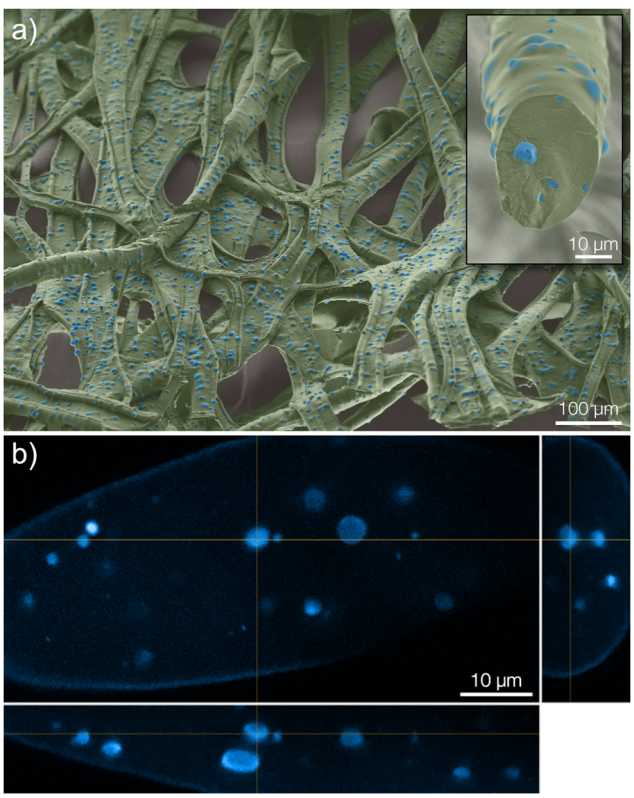

Fig. 2 (a) Colorized scanning electron micrograph visualizing the structure of the nonwoven fiber mesh (green) as well as the PLGA microcapsules (blue) embedded within the fibers. The inset shows a cross-section of a single fiber. (b) Orthogonal projections of confocal micrographs of the same material.

determined. The size distributions of both the fiber and microcapsule (in suspension and fibers) radii were determined from optical micrographs as previously described by us.[27] The size distributions of the three types of fiber materials were found to be similar with fiber radii at around 20 μm (Fig. S1a in the ESI†). Similarity in size was also observed between the microcapsules in aqueous suspension, before introducing them into the fibers, and those later examined in the prepared fibers (radii around 1.5 μm, see Fig. S1b in the ESI†). This meant that the actual process of introducing either microcapsules or dissolved pyrene into the dope solution did not affect the structure of the materials to any observable extent, enabling a direct comparison of release profiles for the different materials.

As can be seen in Fig. 3 there was a significant difference in the release profiles from the different materials. From fibers with a simple surface impregnation of pyrene, a large burst release of about 50% was observed at the first data point after 40 s (0.01 h). Additionally, a very rapid time-dependent release was observed, with a complete release reached after approximately 1 hour. For the samples with bulk impregnated pyrene, an improvement was observed in terms of a significantly lower burst release compared to that of the surface impregnated samples. However, a rapid release was still seen with almost all pyrene released after approximately 20 hours. A considerable decrease in the release rate was observed from fibers where pyrene was encapsulated in microcapsules. From these fibers, a plateau in the release was not reached until after approximately two weeks (300 hours). Adding to this, the observed burst release fraction was negligible. Another benefit of the encapsulation compared to bulk impregnated pyrene, as previously described by us,[18] was the substantial increase in efficiency with regard to fiber uptake of pyrene during preparation.

After approximately three months (2500 hours) in the release medium, there was a distinct change in the appearance of the microcapsules. Before starting the release measurement, the pristine microcapsules were observed as smooth spheres (seen in the insets of Fig. 4 and 1c). However, after three months in the release medium they had started to degrade and fragment, as seen in Fig. 4. A more detailed comparison for microcapsules immersed directly in the aqueous release medium is shown in Fig. S8 in the ESI.† Since the motivation for using polylactides is that the polymer eventually will degrade, this was the intended outcome. Given enough time, the microcapsules would degrade completely, thus preventing the accumulation of microplastics in the environment. No macroscopic changes in the appearance of the fiber materials were however observed over this experimental time frame (see ESI†). At equilibrium in the release measurement, a small amount of pyrene was still seen to be remaining in the microcapsules. This was detected from the fluorescence micrograph in Fig. 4b. A corresponding confocal micrograph of the sample is shown in Fig. S9 in the ESI.† When immersing the fibers in methanol, which is a far better solvent for pyrene compared to the release medium, to leach out the residual pyrene inside the spheres at equilibrium this amount was found to be 3% of the total loading.

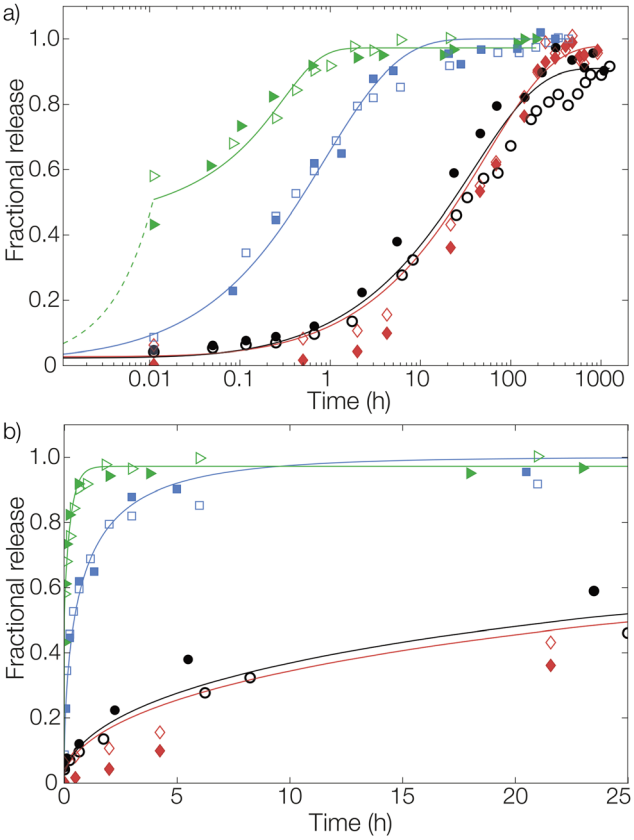

Fig. 3 Fractional release from fibers with pyrene loaded by surface impregnation (▷▶), bulk impregnation (□■), and microencapsulation (◇◆). Release from microcapsules (without fibers) in aqueous suspension (○●) is shown as a comparison. Solid lines are fits to the diffusion models for the corresponding material geometries. In (a) the full release profile is shown on a logarithmic time scale, while in (b) the first 25 hours are shown on a linear time scale. All samples were studied in duplicates, as presented by filled and open symbols, and fitted lines are here shown as averages of individual fits to simplify visualization.

3.3 Effective and apparent diffusion coefficients as tools for assessment of the release properties

Let us finally examine the diffusion models applied to the release data to assess the impact of the encapsulation on the

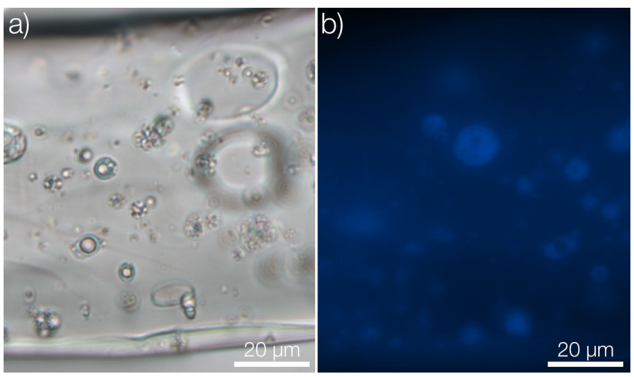

Fig. 4 Fiber segment with embedded microcapsules after more than three months (2500 hours) in aqueous release medium visualized by (a) brightfield and (b) fluorescence microscopy. Insets show the pristine fiber before release measurement.

barrier properties of the fiber material in more detail. The fractional release from the nonwovens and microcapsule suspension was described by Fickian diffusion models in appropriate matrix geometries (sphere, cylinder, or plane sheet).[28] The diffusivity described in these models is not necessarily the true self-diffusion coefficient, but rather an effective diffusion coefficient. Here, the impact of properties such as (micro)porosity inside the matrix and specific interactions between the matrix and active are also included.[14] Presented diffusion models in Fig. 3 were obtained by averaging the fitting parameters from each of the two replicates for all materials. All individually fitted diffusion profiles are presented in the ESI.†

For the composite fibers loaded with microcapsules, the modelled diffusion coefficient D includes – in contrast to the effective diffusion coefficient described previously – diffusional contributions from all compartments of the composite material as well as the distribution of the active between the compartments. This parameter is therefore termed the apparent diffusion coefficient. A comparison of the apparent and effective diffusion coefficients is a powerful tool to investigate the impact of adding different components to a composite material on the release. In addition, the sample geometry used in the model equation can be chosen to monitor the influence of different compartments separately on the diffusion coefficient. In this paper, two different geometrical approaches have been employed to fit the release data as seen in Fig. 5. (1) A cylindrical geometry was used to model the release from cellulosic fibers. Here, the diffusion coefficient is in principle the permeability of the active in the fiber (with or without microcapsules) and consequently a direct measure of the effect of encapsulation on the release. (2) A spherical geometry was used to model the release from the microcapsules. Using this approach, the effect of the surrounding medium (cellulose matrix and aqueous phase for the fiber material or aqueous phase for the microcapsule suspension) on the release from the microcapsules could be investigated. To put this in a slightly different context, approach (2) allowed the rate-determining release properties of the microcapsule to be assessed.

When comparing the apparent diffusion coefficient of the microcapsule-functionalized fibers fitted by a cylindrical geometry to the fitted effective diffusion coefficient in fibers containing bulk impregnated pyrene in Fig. 5, a reduction by almost two orders of magnitude could be observed. As seen in Fig. 3 this corresponded to an increase in the lifetime of the material from hours to more than a week. This was a notable difference, especially considering that the average fiber diameter was around ten times greater than the average microcapsule diameter (Fig. S1 in the ESI†). By employing a simplified steady-state model[29] it was found that microcapsules with radii as small as 30 nm would still be the main rate-limiting barrier, discussed more in detail in the ESI.† When instead comparing the diffusion coefficient for microcapsules embedded within the fibers to those free in aqueous suspension there was only a minor difference in the fitted values. This was a clear indication that the microcapsules acted as the rate-limiting barrier in the release system and that the barrier

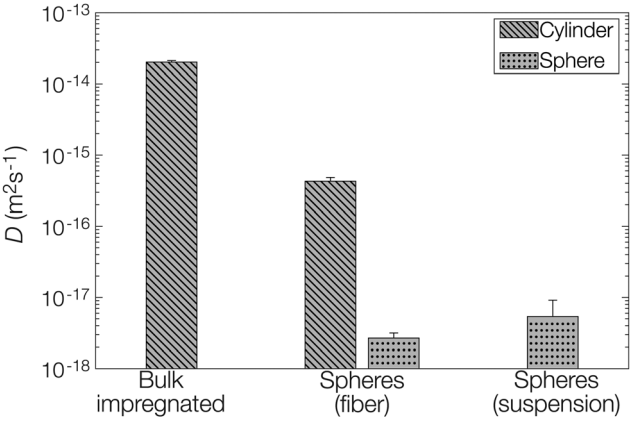

Fig. 5 Fitted diffusion coefficients D from models based on both a cylinder (fiber) and a sphere (microcapsule).

effects of the surrounding fiber were of minor importance in comparison. If this would have not been the case and there was a significant rate-limiting barrier added by the fiber, the fitted effective diffusion coefficient for microcapsules in fibers, fitted on a spherical geometry, would have been significantly smaller than the corresponding value for free microcapsules in aqueous suspension.

Release from the fiber sample with a surface impregnation of pyrene was fitted using a different approach than the one used for bulk impregnation. Two distinct contributions to these release profiles could be seen from the data: an immediate burst release and a diffusive release. During impregnation, a fraction of pyrene was likely also dissolved into the outermost parts of the fiber in addition to the pyrene that was deposited on the outer surface. Therefore, pyrene impregnated onto the fiber surface was released rapidly, resulting in the large burst fraction of around 50% detected at the first measurement after 40 s (0.01 h). This burst was here assumed to be of zero-order kinetics (simply due to lack of data points) for mathematical modelling, shown by the dashed line for surface impregnated pyrene in Fig. 3. The diffusive part of the release was significantly slower. This part was modelled as diffusion from a plane sheet with the same effective diffusion coefficient as the sample containing bulk impregnated pyrene. Hence, the diffusion coefficient was not fitted for this material. Instead, this allowed us to determine the thickness of the pyrene-containing layer to 7 μm, which was about half of the average fiber radius.

4. Conclusions

To conclude, we have presented a new concept where microcapsules provide long-term controlled release from fiber materials, as exemplified by cellulosic nonwovens in this contribution. More importantly, the sustained release is also predictable since the release rate is exclusively determined by the rate-limiting microcapsules. This can be put in contrast to recent work on sustained release fiber materials where functional lifetimes on the order of a handful of days are commonly

observed and where the release depends to a high extent on the fiber material and not exclusively on the delivery vehicle.[30,31] Wound care is an application area where the functional lifetime achieved by the nonwovens presented in this paper is particularly suitable. Antimicrobial wound dressings typically lose their effect after a few days due to the fast release as discussed in the introduction. Implementation of our sustained release concept would lead to less frequent wound dressing changes, and as a consequence reduced suffering for the patients. In addition, the microcapsule formulation could be combined with impregnation (with a significantly faster release) to rapidly reach the minimum efficient concentration in order to avoid exposing the microflora to antimicrobial levels that could select for resistance development. In applications where longer functional lifetimes are desired, such as agricultural textiles, the release properties could be further optimized by tailoring the size distribution of microcapsules. From a product point of view, the concept of microcapsule functionalization is a means for resource-efficient and sustainable use of actives since the materials can be used for longer periods, with lower total loadings and emissions of actives that otherwise could pollute the environment. We are currently implementing this concept for long-term infection control by sustained release of antimicrobial agents.

Author contributions

V. E.: conceptualization, methodology, formal analysis, investigation, data curation, writing – original draft, visualization. J. M.: methodology, investigation. T. Y. N.: methodology, investigation. M. A. T.: conceptualization, methodology, writing – review & editing, supervision, project administration, funding acquisition. L. E.: conceptualization, methodology, writing – review & editing, supervision, project administration, funding acquisition.

Conflicts of interest

There are no conflicts to declare.

Acknowledgements

The Swedish Research Council FORMAS (2018 – 02284) and Vinnova (2017 – 04693 and 2021 – 01611) are acknowledged for funding. We thank Dr Mats Hulander for SEM micrographs and Dr Katarina Logg for the confocal micrographs. Dr Johan Svenson and Dr Therese Andersson are acknowledged for cytotoxicity tests.

References

1 J. L. Harding and M. M. Reynolds, *Trends Biotechnol.*, 2014, **32**, 140–146.
2 S. Freiberg and X. X. Zhu, *Int. J. Pharm.*, 2004, **282**, 1–18.
3 I. Fitridge, T. Dempster, J. Guenther and R. De Nys, *Biofouling*, 2012, **28**, 649–669.
4 D. M. Yebra, S. Kiil and K. Dam-Johansen, *Prog. Org. Coat.*, 2004, **50**, 75–104.
5 B. Liu, Y. Wang, F. Yang, X. Wang, H. Shen, H. Cui and D. Wu, *Colloids Surf., B*, 2016, **144**, 38–45.
6 P. Gilbert and A. J. McBain, *Clin. Microbiol. Rev.*, 2003, **16**, 189–208.
7 F. A. Guardiola, A. Cuesta, J. Meseguer and M. A. Esteban, *Int. J. Mol. Sci.*, 2012, **13**, 1541–1560.
8 M. Manzano and M. Vallet-Regí, *Adv. Funct. Mater.*, 2020, **30**, 1902634.
9 B. G. Trewyn, S. Giri, I. I. Slowing and V. S.-Y. Lin, *Chem. Commun.*, 2007, 3236–3245.
10 C. Wischke and S. P. Schwendeman, *Int. J. Pharm.*, 2008, **364**, 298–327.
11 B. K. Lee, Y. Yun and K. Park, *Adv. Drug Delivery Rev.*, 2016, **107**, 176–191.
12 R. P. Babu, K. O'Connor and R. Seeram, *Prog. Biomater.*, 2013, **2**, 8.
13 J. M. Anderson and M. S. Shive, *Adv. Drug Delivery Rev.*, 1997, **28**, 5–24.
14 M. Andersson Trojer, L. Nordstierna, J. Bergek, H. Blanck, K. Holmberg and M. Nydén, *Adv. Colloid Interface Sci.*, 2015, **222**, 18–43.
15 Y. Yeo, T. Ito, E. Bellas, C. B. Highley, R. Marini and D. S. Kohane, *Ann. Surg.*, 2007, **245**, 819–824.
16 U. Bhardwaj, R. Sura, F. Papadimitrakopoulos and D. J. Burgess, *Int. J. Pharm.*, 2010, **384**, 78–86.
17 R. Paul, *High Performance Technical Textiles*, John Wiley & Sons, 2019.
18 H. Ulmefors, T. Yang Nilsson, V. Eriksson, G. Eriksson, L. Evenäs and M. Andersson Trojer, *Macromol. Mater. Eng.*, 2022, **307**, 2200110.
19 D. Klemm, B. Heublein, H.-P. Fink and A. Bohn, *Angew. Chem., Int. Ed.*, 2005, **44**, 3358–3393.
20 C. Olsson and G. Westman, *Direct Dissolution of Cellulose: Background, Means and Applications*, InTech, 2013.
21 M. W. Frey, *Polym. Rev.*, 2008, **48**, 378–391.
22 D. Crespy, K. Friedemann and A.-M. Popa, *Macromol. Rapid Commun.*, 2012, **33**, 1978–1995.
23 A. Kakoria and S. Sinha-Ray, *Fibers*, 2018, **6**, 45.
24 K. Jedvert, A. Idström, T. Köhnke and M. Alkhagen, *J. Appl. Polym. Sci.*, 2020, **137**, 48339.
25 T. Y. Nilsson and M. A. Trojer, *Soft Matter*, 2020, **16**, 6850–6861.
26 J. Bergek, M. Andersson Trojer, A. Mok and L. Nordstierna, *Colloids Surf., A*, 2014, **458**, 155–167.
27 V. Eriksson, M. A. Trojer, S. Vavra, M. Hulander and L. Nordstierna, *J. Colloid Interface Sci.*, 2020, **579**, 645–653.
28 J. Crank, *The mathematics of diffusion*, Oxford University Press, 1979.
29 M. A. Trojer, H. Andersson, Y. Li, J. Borg, K. Holmberg, M. Nydén and L. Nordstierna, *Phys. Chem. Chem. Phys.*, 2013, **15**, 6456–6466.
30 H. He, M. Wu, J. Zhu, Y. Yang, R. Ge and D.-G. Yu, *Adv. Fiber Mater.*, 2022, **4**, 305–317.
31 M. S. El-Okaily, A. M. El-Rafei, M. Basha, N. T. Abdel Ghani, M. M. H. El-Sayed, A. Bhaumik and A. A. Mostafa, *Int. J. Biol. Macromol.*, 2021, **182**, 1582–1589.